

LASER INTERFEROMETER GRAVITATIONAL WAVE OBSERVATORY
- LIGO -
CALIFORNIA INSTITUTE OF TECHNOLOGY
MASSACHUSETTS INSTITUTE OF TECHNOLOGY

Technical Note	LIGO-T070228-00-Z	2007/09/13
Search for a Diurnal Variation of the Power detected at the fsr frequency		
C. Forrest, T. Fricke, S. Giampanis and A.C. Melissinos		

Circulation restricted to LIGO Science Collaboration

California Institute of Technology
LIGO Project, MS 18-34
Pasadena, CA 91125
Phone (626) 395-2129
Fax (626) 304-9834
E-mail: info@ligo.caltech.edu

Massachusetts Institute of Technology
LIGO Project, Room NW17-161
Cambridge, MA 02139
Phone (617) 253-4824
Fax (617) 253-7014
E-mail: info@ligo.mit.edu

WWW: <http://www.ligo.caltech.edu/>

Search for a Diurnal Variation of the Power detected at the fsr frequency

C. Forrest, T. Fricke, S. Giampanis and A.C. Melissinos

for the LIGO stochastic analysis group

University of Rochester

2007/09/13

1 Motivation

The AS_Q channel of the LIGO interferometers is being read out not only at 16 kHz, but also at the high sampling rate of 232 kHz. This makes it possible to measure the spectrum at the free spectral range (fsr), $f = 37.52$ kHz for the 4 km IFO's. The spectrum obtained for H1 during the S5 run shows a strong enhancement at the fsr, similar to that which would be generated by a signal with a broadband flat spectrum in that frequency region. The enhancement is slightly asymmetric indicating that it is driven, in part, parametrically by a nearby mechanical resonance.

To test whether the observed signal is of astrophysical origin, as contrasted to noise, we can consider the case where the signal comes from one or more discrete sources in the sky. In that case the signal should contain the harmonics of the daily sidereal frequency. The modulation of the signal is more pronounced at the fsr frequency than at the canonical gravitational band because the lobes of the antenna pattern are narrower. As a result, however, for an incident wave of given strain, the averaged signal strength at the fsr is reduced by a factor of ~ 5 as compared to its value at ~ 100 Hz.

A diurnal variation need not necessarily be of astrophysical origin. Since we have more than one year of data we are able to distinguish solar from sidereal frequencies. As shown below there is a very strong first and second harmonic of the solar period present in the data. We think that these harmonics are due to the “tidal correction” that is applied in order to keep the IFO in lock. At the higher frequencies one can find relevant sidereal harmonics but the spectrum is too noisy to allow unambiguous identification.

In the absence of a signal we can set upper limits on the gravitational flux from a particular direction in the sky. We have simulated the signal from the galactic center and from Sco-X1 and present the corresponding limits. These limits are weaker than those obtained by the radiometer search [1], but they refer, of course, to a completely different frequency range.

2 Data analysis

We calculate the power in the fsr region integrated over a finite frequency band Δf . We do this by applying a filter to the measured power spectrum and integrating from -200 to

+200 Hz around $f_0 = 37.520$ kHz. A typical power spectrum is shown in Figure 1 where the

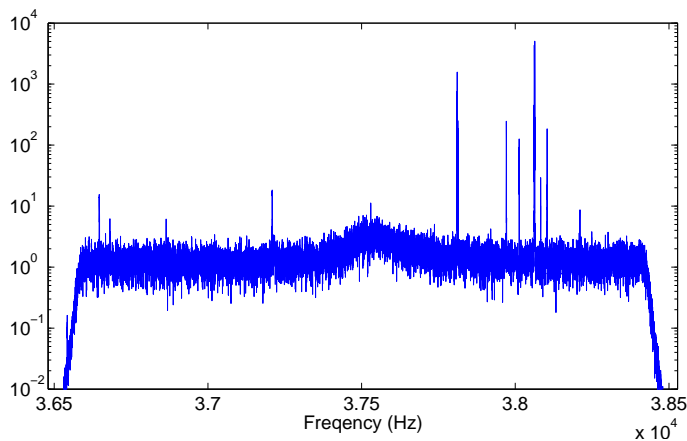


Figure 1: Typical power spectral density at the fsr.

ordinate is in $(\text{counts})^2/\text{Hz}$, and the frequency binwidth is $BW = 0.125$ Hz [2]. The filter is the inverse of the interferometer transfer function squared and has a FWHM = 180 Hz. It is normalized to unity at f_0 as shown in Figure 2. The integrated power is calculated for

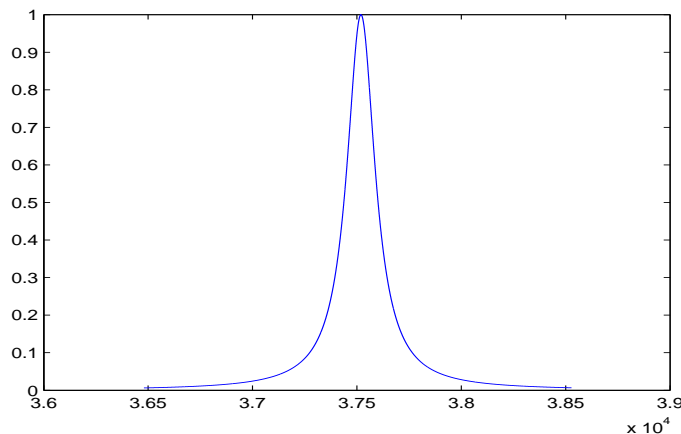


Figure 2: The filter used when integrating the power spectral density at the fsr.

each frame, of 64 s duration.

A plot of the integrated power vs gps time for the period July-December 2006 is shown in Figure 3, and in the inset for a two day period. By inspection we see that the integrated power varies at the diurnal and twice daily frequencies. To find the frequency content of this time series we use the Lomb-Scargle (L-S) algorithm [3] to form the periodogram. The data were selected when the interferometer was in lock and data points deviating by more than 3σ from the mean were excluded. In addition we exclude certain periods of time when the signal power was significantly different from its mean value. The selected data sample is shown in Figure 4. The calibration factors $\alpha(t)$ have not been included.

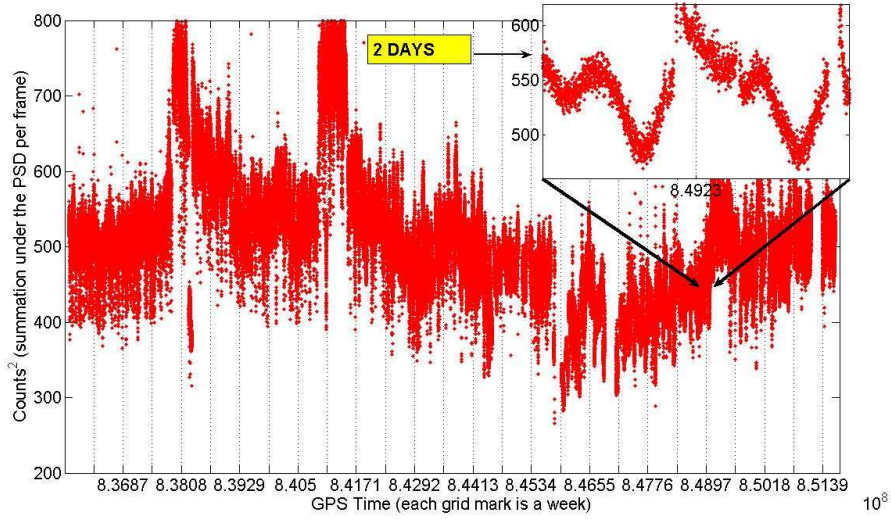


Figure 3: Time series of integrated power for the period July-December 2006.

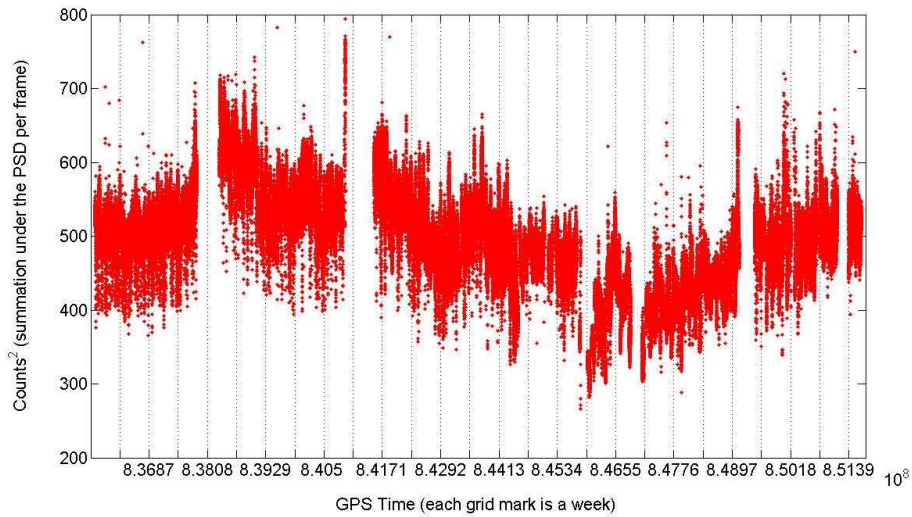


Figure 4: Time series of integrated power for the period July-December 2006, after cuts.

The advantage of the L-S algorithm is that it can handle discontinuous time series as well as non equally sampled data. It returns the power in the one sided spectrum, and can be oversampled to give frequency resolution exceeding $1/T$, with T the total duration of the record. The modulation amplitude of the signal at a particular frequency is related to the power in the periodogram through

$$X_0 = 2 \left(\frac{\text{Power} \times \text{variance}}{N} \right)^{\frac{1}{2}} \quad (1)$$

In the above equation N is the number of frequencies examined, namely the number of points in the time series which equals $N = 1.80519 \times 10^5$ for six months of data. The variance of the data sample is $\sigma^2 = 3772$. The total duration of the record is $T = 1.5897 \times 10^7$ s. The frequency binwidth is $BW = 1.57 \times 10^{-8}$ Hz, because we are oversampling by a factor of 4. We are examining frequencies only up to $\sim 7 \times 10^{-4}$ Hz.

For clarity the frequency spectrum is shown in three different regions

Figure 5: $(0-3) \times 10^{-6}$ Hz

Figure 6: $(1-3) \times 10^{-5}$ Hz

Figure 7: $(3-10) \times 10^{-5}$ Hz

The red vertical lines indicate the harmonics of the sidereal frequency. Figure 5 shows the lowest frequency range (the DC component has been removed). It is dominated by a frequency $f = 6.29 \times 10^{-8}$ Hz, which corresponds to a period of 184 days. This slow modulation is also apparent in the data and if it persists in the entire sample it may have physical significance. The next frequency band, shown in Figure 6, contains the three pronounced lines

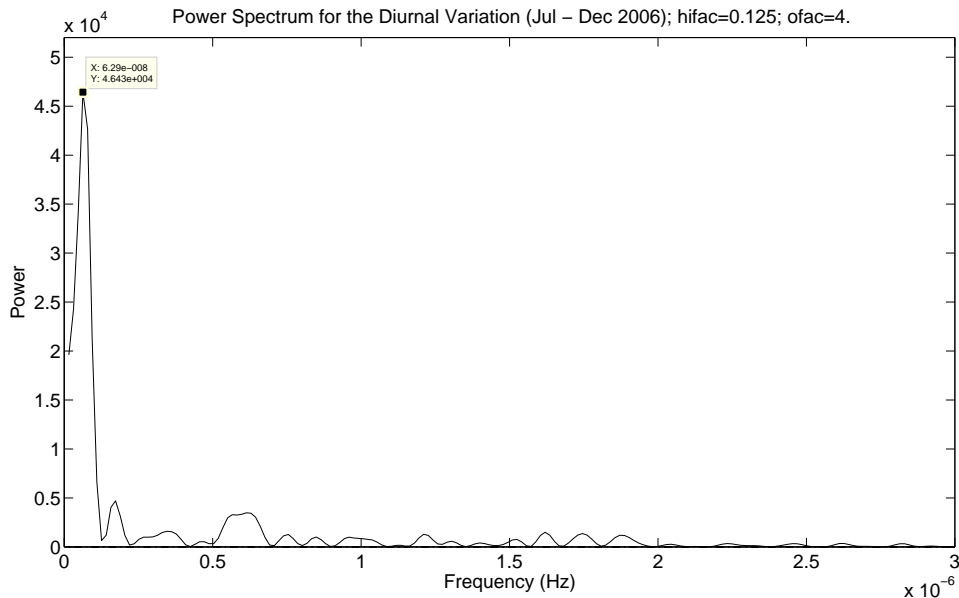


Figure 5: Frequency spectrum of the integrated power in the range 0 to 3×10^{-6} Hz.

in the spectrum. They are located at

$f = 1.157 \times 10^{-5}$ Hz. Period of exactly one solar day.

$f = 2.237 \times 10^{-5}$ Hz. This is not an identifiable frequency except that it differs from the next peak (twice daily frequency) by 7.8×10^{-7} Hz, which corresponds to a period of 14.8 days and could be related to the lunar cycle.

$f = 2.315 \times 10^{-5}$ Hz. Period of exactly half a solar day.

Figure 7 shows a dense spectrum of lines extending up to 10^{-4} Hz. For this data sample, lines with power $P > 16$ have a “false alarm” probability less than 10^{-3} and are therefore

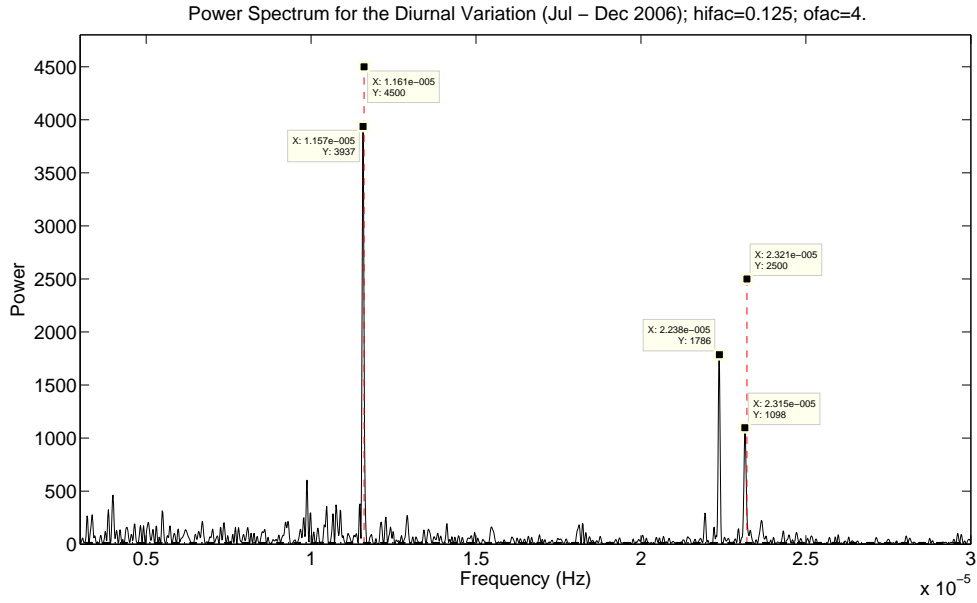


Figure 6: Frequency spectrum of the integrated power in the range 10^{-5} to 3×10^{-5} Hz.

statistically significant. In the region shown in Figure 7 the spectrum is “noisy” due to a lack of smoothness of the input data and masks any harmonics of comparable power that may be present. To calculate the power at a particular frequency of the periodogram we sum the

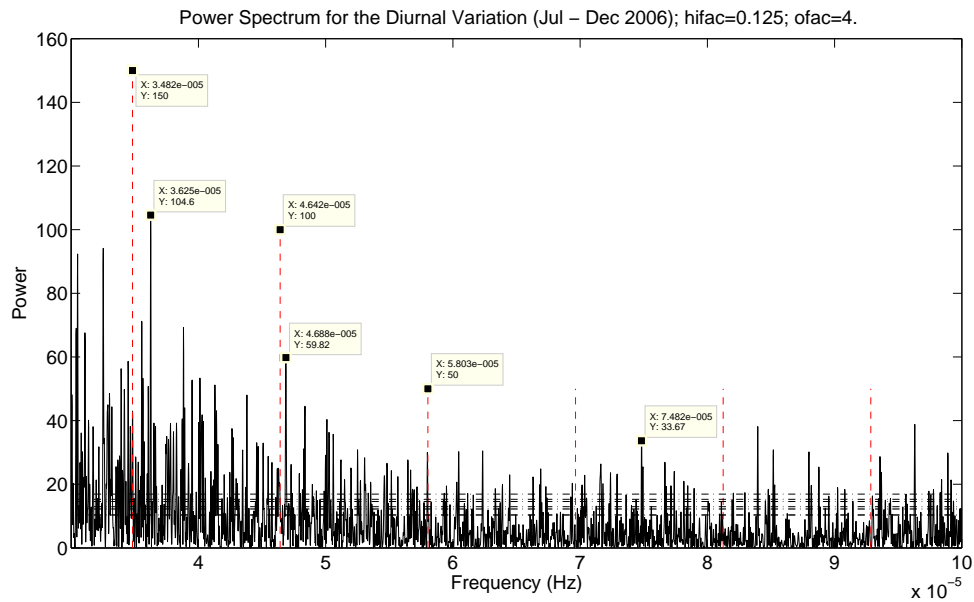


Figure 7: Frequency spectrum of the integrated power in the range 3×10^{-5} to 10^{-4} Hz.

power over ± 5 bins around the peak (and divide by the oversampling factor) and use Eq.(1) to find the harmonic amplitude X_0 in (counts)². This can be converted to (strain)²/Hz from

the known calibration value at the fsr and of the integration bandwidth Δf ,

$$(\text{strain})_{n/\text{Hz}}^2 = \frac{1}{|C(0)|^2} \frac{X_{0,n}}{\Delta f} \quad (2)$$

where $\Delta f = 180$ Hz as determined by the filter. For S5 we have $C(0) = 4 \times 10^{21}$ counts/strain. From the data we obtain the following strain densities

$n = 1$	$f = 1.157 \times 10^{-5} \text{Hz}$	$ h _n^2 = 6.6 \times 10^{-45} / \text{Hz}$
$n = 1.92$	$= 2.237 \times 10^{-5} \text{Hz}$	$= 4.5 \times 10^{-45} / \text{Hz}$
$n = 2$	$= 2.315 \times 10^{-5} \text{Hz}$	$= 3.8 \times 10^{-45} / \text{Hz}$
$n = 3$	$= 3.482 \times 10^{-5} \text{Hz}$	$= 8.0 \times 10^{-46} / \text{Hz}$
$n = 4$	$= 4.642 \times 10^{-5} \text{Hz}$	$< 6.3 \times 10^{-46} / \text{Hz}$
$n = 5$	$= 5.803 \times 10^{-5} \text{Hz}$	$= 6.6 \times 10^{-46} / \text{Hz}$
$n = 6$	$= 6.693 \times 10^{-5} \text{Hz}$	$< 2.6 \times 10^{-47} / \text{Hz}$

At $n = 3$ and $n = 5$ the data show peaks and we give the corresponding power; as discussed later we believe that these are accidental peaks. At $n = 4$ and $n = 6$ there are no peaks and we give upper limits. Note that for $n = 3$ to $n = 6$ the harmonics are evaluated at the **sidereal** frequency.

3 Results

We begin by calculating the power expected at the fsr from a source fixed in the sky, assuming that the gravitational wave is unpolarized and the strain at the IFO is $h_{\times} = h_{+} = 1/\sqrt{2}$. We decompose the resulting time series into its harmonic components and compare them to the observational data to find (or limit) the gravitational energy flux reaching the IFO. The results for two directions in the sky, the galactic center and Sco-X1, are given in the following table. For each harmonic the second (and fourth) column give the result of the simulation, the third (and fifth) column are obtained by dividing the measured strain by the simulation to obtain the total strain due to that source. The $n = 0$ entry refers to the expected average value of the simulation. Sources in the galactic plane give similar spectra depending on their galactic right ascension.

	galactic center		Sco-X1	
	simulation	$ h ^2/\text{Hz}$	simulation	$ h ^2/\text{Hz}$
$n = 0$	0.0281		0.0269	
$n = 1$	0.0156	$4.2 \times 10^{-43} / \text{Hz}$	0.0136	$7.4 \times 10^{-43} / \text{Hz}$
$n = 2$	0.0044	$8.6 \times 10^{-43} / \text{Hz}$	0.0105	$3.6 \times 10^{-43} / \text{Hz}$
$n = 3$	0.0259	$3.1 \times 10^{-44} / \text{Hz}$	0.0206	$3.9 \times 10^{-44} / \text{Hz}$
$n = 4$	0.0118	$< 5.3 \times 10^{-44} / \text{Hz}$	0.0095	$< 6.6 \times 10^{-44} / \text{Hz}$
$n = 5$	0.0034	$19 \times 10^{-44} / \text{Hz}$	0.0004	
$n = 6$	0.0042	$< 6.2 \times 10^{-44} / \text{Hz}$	0.0090	$< 2.9 \times 10^{-44} / \text{Hz}$

Circulation restricted to LIGO Science Collaboration

In a self-consistent picture all harmonics should give the same value for the strain due to a given source (column 3 or column 5). This is not the case and we know that the $n = 1$ and $n = 2$ entries should not be used because they are not at the sidereal frequency. Combining the remaining entries we can set a conservative upper limits on the strain

$$\begin{aligned} \text{From the galactic center} &< 8.4 \times 10^{-44}/\text{Hz} \\ \text{From Sco - X1} &< 4.5 \times 10^{-44}/\text{Hz} \end{aligned}$$

We can express the above results in terms of the detected gravitational energy density per unit frequency interval at $f_0 = 37.52$ kHz normalized to the critical energy density

$$\frac{1}{\rho_c} \frac{d\rho_G}{df} = \frac{20\pi^2}{3H_0^2} f^2 |h|^2 = 1.8 \times 10^{46} |h|^2 \quad (3)$$

In Eq.(3) we used $H_0 = 0.72 \times (10^{10} \text{ years})^{-1}$. The gravitational energy flux is obtained from Eq.(3)

$$F = \left[\frac{1}{\rho_c} \frac{d\rho_G}{df} \right] c \rho_c \Delta f = \frac{5 \pi^2 c^3}{2 G} f^2 |h|^2 \Delta f = 1.4 \times 10^{49} |h|^2 \Delta f \quad \text{ergs}/(\text{cm}^2 - \text{s}) \quad (4)$$

4 Discussion

We would like to know the origin of the three prominent lines in the spectrum, namely at $n = 1$, $n = 1.92$ and $n = 2$ times the solar daily frequency. To compensate for the effect of the Earth tides both the frequency of the carrier and the position of the end test masses are modulated [4]. The signal that drives the test masses is the ‘‘Tidal Servo’’ and it is recorded during the run. We spectrally analyzed the tidal servo signal for the two month period Dec. 2006 and Jan. 2007 and the result is shown in Figure 8. This spectrum can be directly compared to that of the data shown in Fig. 6. The spectra are not identical but have similar features. The calibration data $\alpha(t)$ also exhibit some diurnal variation. The spectrum of $\alpha(t)$ for the month of December is shown in Figure 9 in the same frequency band. The once daily frequency is again present but at a much lower modulation level. Finally we examined the ASQ channel and the resulting spectrum is shown in Figure 10. Below we summarize the observed modulation at the once daily solar frequency in the three channels that we examined

Channel	Modulation
ASQ	$\pm 3\%$
$\alpha(t)$	$\pm 1\%$
1 fsr	$\pm 11\%$

The most probable conclusion is that the optical gain is affected by the tidal servo, and that this effect is amplified at the 1 fsr. For instance the recycling cavity gain is certainly

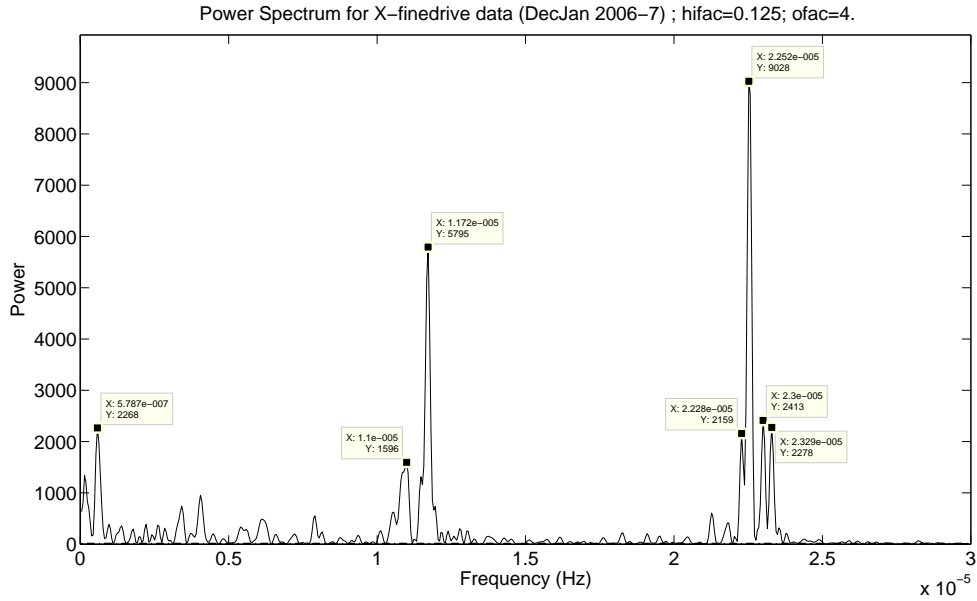


Figure 8: Frequency spectrum of the tidal servo (X-finedrive) signal for the period December 2006 through January 2007

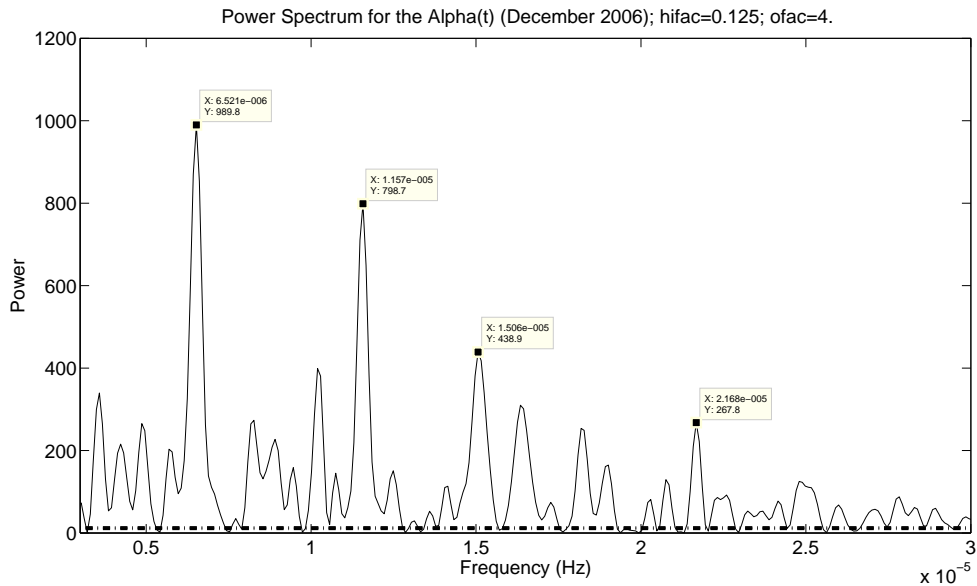


Figure 9: Frequency spectrum for $\alpha(t)$ coefficients for December 2006

dependent on small changes in the carrier frequency, and this in turn would affect the optical gain.

Next we wish to address the possible presence of higher harmonics. As already mentioned the probability that a line in the L-S spectrum with Power > 16 is a statistical fluctuation is less than 10^{-3} . However the number of such statistically significant lines in the range $(3 - 10) \times 10^{-5}$ Hz is ~ 150 , or a line density of 2.14×10^6 lines/Hz. When we search

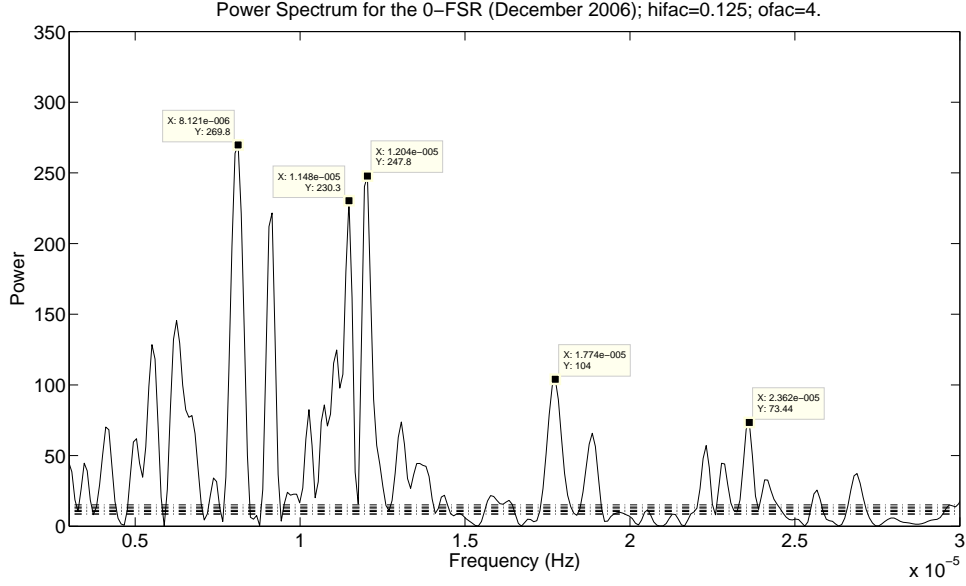


Figure 10: Frequency spectrum for the integrated power in the AS-Q channel

for a harmonic we accept a peak in the narrow interval $\delta f = 6.3 \times 10^{-7}$ Hz, so that the mean accidental rate for locating one harmonic in δf is $P_1(\delta f) = .34$. We searched for four harmonics and located two of them, $n = 3$ and $n = 5$. The random (Poisson) probability of such an occurrence is 23%. Thus we can not claim the presence of harmonics in the data.

For an estimate of the numerical magnitude of the results, we assume an emission bandwidth of ~ 1 kHz at $f = 37.5$ kHz and integrate the gravitational flux over a sphere centered on the source which is at a distance of ~ 8 kpc. The resulting luminosity in gravitational waves is

$$\text{Galactic center} \quad L_G = 9.4 \times 10^{54} \text{ ergs/s} \simeq 10^{15} L_{\text{galaxy}}$$

which is clearly un-physical. If instead of the flux we consider the energy density in gravitational waves in a similar bandwidth of 1 kHz we obtain for the galactic center

$$\rho_G = 1.5 \times 10^{-2} \text{ ergs/cm}^3 = 1.5 \times 10^6 \rho_c$$

This is a completely unacceptable energy density in terms of the nucleosynthesis bound. As a point of reference the energy density in the galactic halo [5] is

$$\rho_{\text{halo}} = (2 - 13) \times 10^{-4} \text{ ergs/cm}^3$$

To improve the data analysis it is necessary to reduce the density of spectral lines, that carry significant power, in the region above the 2nd harmonic. Towards this goal we will include

the $\alpha(t)$ coefficients, attempt a tighter σ cut, and examine the effect of smoothing the high frequency components in the data (by downsampling).

5 References

- 1 B. Abbott et al. “Upper limit map of a background of gravitational waves” (DA10473) accepted for publication in Physical Review D.
- 2 “The High-Frequency Stochastic Search (S4): An Update for the March 2007 LSC Meeting - LIGO/VIRGO Scientific Collaborations Meeting”, March 19-22, 2007, LIGO internal report G070057-00-Z.
- 3 W.H.Press, B.P.Flannery, S.A.Teukolsky and W.T.Vetterling “Numerical Recipes in C: The Art of Scientific Computing” Cambridge 1990; J.D.Scargle Ap. J. **263**, 835 (1982); J.H.Horne and S.L.Baliunas Ap. J. **302**, 757 (1986).
- 4 F.Raab and M.Fine “ The Effect of Earth Tides on LIGO Interferometers” LIGO-T970059-01-D (1997); E.Morganson “ Developing an Earth-Tides Model for LIGO Interferometers”, LIGO-T990181-00-W (1999).
- 5 E.W.Kolb and M.S.Turner “The Early Universe” Addison Wesley/Westview Press, 1990.